Continuous-Time Optimization of Integrated Networks of Electricity and District Heating Under Wind Power Uncertainty

Ramin Nourollahi[a], Kazem Zare*[,a], Behnam Mohammadi-Ivatloo[a], Vahid Vahidinasab[b], Amjad anvari moghadam[c]

[a] *Faculty of Electrical and Computer Engineering, University of Tabriz, Tabriz, Iran*
[b] *Department of Engineering, School of Science and Technology, Nottingham Trent University, Nottingham NG11 8NS, UK*
[c] *Department of Energy (AAU Energy), Aalborg University, Aalborg, Denmark*

Abstract

The integrated operation of the electricity and district heating systems (EDHS) attracted lots of attention in recent years due to considerable impacts on the power system's flexibility. The time intervals and mathematical methods used in the optimization procedure are essential, especially when flexible operation in the presence of intermittent renewable resources is an objective because of the sub-hourly dynamics. Due to the intrinsic deficiencies of the traditional discrete-time hourly models in handling the sub-hourly variation of the load and renewable generation, in this paper, a new continuous-time optimization model is proposed to model the look-ahead operation of EDHS. The proposed continuous-time model is approximated by the linear spline-based trajectories and represented by the cubic splines of Bernstein function space to capture EDHS's sub-hourly load and wind generation fluctuations. The EDHS of Barry Island is employed to investigate the proposed model and obtain results compared with the discrete-time procedure. Also, to measure the impact of uncertainties on both the continuous-time and discrete-time models, the information

*Corresponding author
Email addresses: Ramin.nourollahi@tabrizu.ac.ir (Ramin Nourollahi), kazem.zare@tabrizu.ac.ir (Kazem Zare*), Bmohammadi@tabrizu.ac.ir (Behnam Mohammadi-Ivatloo), vahid.vahidinasab@ntu.ac.uk (Vahid Vahidinasab), aam@et.aau.dk (Amjad anvari moghadam)

gap decision theory (IGDT) is utilized. The examination results illustrate that the proposed continuous-time model brings a saving of 0.91% in the costs when compared with the discrete-time model on a small test system. In addition, the results of the IGDT technique show more opportunities by wind increasing and fewer threats by wind reduction using the proposed continuous-time optimization problem compared to the discrete-time model.

Keywords: Continuous-time optimization, Bernstein polynomials, integrated electricity and district heating system, uncertainty, information gap decision theory.

Nomenclature

A. Indices

h	Index of energy hub
r	Index of energy storage
t	Time index [hour]
d	Index of sub-hourly time interval
q	Index for degree of Bernstein function
i, j, k	Index of electricity network bus
n, p	Node and pipeline's index of district heating network

B. Superscripts

RES	Renewable energy system index
CHP	Combined heat and power unit index
DA	Day-ahead index
EH	Energy hub index
HP	Heat pump index
Dn, Up	Reserve up and down

C. Parameters and constants

C^{NG}, HV	Gas price and heat value of natural gas [\$/m^3], [$Mcal/m^3$]
η^{Ch}, η^{dch}	Charging and discharging efficiency [%]
$\eta^{CHP/CHP,L}$	CHP unit's electrical/loss efficiency [%]
COP^{HP}	Performance coefficient of heat pump
P^{RES}	Generated power of renewable sources [MW]
P^L, Q^L, H^L	Active load, reactive load, and heat load [MW]
r_{ij}/x_{ij}	Resistance and reactance between buses i, j [Ω]
T^{Amb}, V_0	Ambient temperature and slack bus voltage [$^\circ C$], [$p.u$]
$m^L/m^S, m$	Rate of load/source, and pipeline mass flow [kg/s]
L	Pipeline's length [m]
λ	Coefficient of heat transfer in pipeline

D. Variables

B	Representing the Bernstein coefficient of all variables
$P_{DA,CHP}$	Traded power of units in day-ahead market[MW]
P_{ij}/Q_{ij}	Active and reactive power bus i to j[MW]
P^G/H^G	Active and reactive generated power [MW]
P^{EH}/H^{EH}	Electric and heat power of energy hub [MW]
P^{HP}	Electric power of heat pump [MW]
H^S, H^R	Heat load and heat source [MW]
R^{Up}, RDn	Reserve power of CHP units [MW]
E	Energy of the storage[MWh]
δ^{ru}, δ^{dn}	charge and discharge power storage in reserve [MW]
d, g	Charging and discharging power of storage s [MW]
V	Magnitude of Voltage [p.u]
T^S/T^R	Supply/return temperature [$^\circ C$]

T^{in}/T^{out}	Input/output temperature of pipelines $[^{\circ}C]$
T^{mix}	Temperature of mixture node $[^{\circ}C]$

1. Introduction

Wind power generators (WPGs) with a relatively large share among the renewable energy resources plays an important role in the operation of the power systems [1, 2]. The sub-hourly variation of the wind power generation and the uncertainnature of WPGs is a critical challenge for the power system operators [3, 4]. Besides, the fast-variation nature of WPGs has led to the need for flexibility services to mitigate the sub-hourly and rapid alternations of them [5, 6]. It should be mentioned that the variation magnitude and generated power of the wind producers in an area depends on various parameters like dimensions and geographical location of turbines[7, 8].

1.1. Literature review

System operators choose various approaches in different countries to deal with the challenges of the WPGs. The simple solution of system operator to deal with these challenges is the wind power curtailment [9]; however, this solution is not the system operator's priority. An alternate solution that enables the maximum usage of renewable generation, is to take a holistic approach to energy by integrating electricity with other vectors of energy [10]. For instance, integration of the electricity network with the district heating facilities, including combined heat and power (CHP), electric boilers, and heat pumps is one of the potential integrated approaches that increase the flexibility of operation by taking the advantage of both the networks [11]. Due to the restrictions of the heat generation by CHP units, the wind power variation may not be compensated entirely by the CHP units [12]. Thus, the insufficient flexibility options would result to more renewable energy curtailment that is unnecessary [13, 14]. In [15], an aggregated model is considered for buildings to optimize the day-ahead operation of integrated electricity and district heating network to accommodate

the wind power and reduce the wind curtailment by using the building's thermal inertia. The wind power curtailments are also investigated in [16] by utilization of energy storage devices in the district heating and power systems. Besides, the joint hourly commitment of the heat exchange station and the generation units of the combined heat and power systems is proposed in [17] to reduce the wind power curtailment and the system's operation cost. The energy storage system are deemed as a secure and appointed proposal for providing the flexibility requirements especially in the sub-hourly markets [18]. The power-to-heat facilities in district heating system is proposed as the a resource to increase the flexible resource for increasing the penetration of the renewable resources in [19]. In [20], the electricity used for heating is investigated as a low-carbon option to increase the power system flexibility for integration of variable renewable resources.

Since the mentioned challenges and solutions are investigated by the ancillary service markets, the energy and co-optimization of the reserve market are required to investigate the wind variability due to the sub-hourly variations [21]. Generally, the potentials of the district heating systems on the flexibility in the electricty markets is reviewed in [22]. In [23], energy and reserve markets are co-optimized for the unit commitment problem to overcome the variable wind energy generations in a real electricity and district heating system. The reserve markets are entirely investigated in [24], to improve the economic efficiency of the energy system through the energy co-optimization, in which the variation of WPG is investigated by the district heating system in the reserve market. In [25], using the bi-level optimization, co-optimization of the district heating system integrated with a electric system is investigated to obtain the strategic operation in energy and reserve markets.

Modeling the uncertainties in the heating and renewable-based power systems could affect the economic efficiency of the system. Different methods are proposed in the literature to investigate the uncertainties. The robust optimization approach is one of the well-known uncertainty modeling methods used when the

bounds of uncertain parameters are known. In [26]–[27] robust optimization is proposed to schedule the power and district heating systems to hedge against the uncertainties in short-term operations. Stochastic programming is another uncertainty modeling method s proposed in [28], [29] to model the uncertainties of power market price, wind generation, and solar irradiation with the coordinated operation of CHP generators in a microgrid. Since the probabilistic distribution of the uncertain parameters is unknown in some cases, the distributionally robust optimization approach is also another new method that has applied in the literature to model the uncertainties. In [30], [31], distributionally robust optimization is applied to the conventional unit commitment problem to model the wind generation uncertainty in the energy and reserve markets. In order to model the probabilistic energy flow, in [32] the Monte Carlo simulation and point estimate method are used to consider the uncertainties of the heating and power systems. Also, the interval optimization is proposed in [33] to get the optimal scheduling of the integrated EDHS, in which the dynamic characteristics of the heating network are considered for more integration of the wind power. Other methods like the artificial neural network and evolutionary algorithms are some of the famous methods used in this field [34, 35].

In the above studies, the integration of electricity and district heating networks without mainly considering the fast variations of WPGs has only been represented via an the hourly discrete-time mathematical formulation.However, the hourly discrete-time method considers only the hourly commitments of the resources and the hourly ramping of the flexible resources such as boilers, storage systems, and CHPs. Because of the sub-hourly deviation of the WPGs and weakness in the sub-hourly modeling of wind deviations in hourly modeling, the conventional hourly discrete-time model would not be proper for the renewable-based (mainly wind-based) energy systems. In order to address the weakness of the discrete-time hourly modeling method, the continuous-time modeling based on Bernstein polynomial functions is proposed in the literature. By using the mentioned continuous-time method, the sudden sub-hourly deviations of the WPGs can be handled by sub-hourly modeling the ramping capabilities

of the resources in the combined power and district heating resources. Also, the continuous-time modeling helps to enhance the coordinated operation of electricity and heating networks to handle sudden variation of the WPGs and loads.

Recently, only a few studies have focused on continuous-time optimization of power system problems. Originally, continuous-time optimization was used to precisely quantify the cost of ramping shortages in thermal systems with a high proportion of renewable energy output, such as the California power system [36]. In lieu of the conventional piece-wise constant formulation, ramping limits may be added directly to the derivatives of the decision variables once they have been permitted to be continuous and smooth functions of time. The continuous-time model restricts the decision variables to polynomials of degree r, allowing them to be represented as Bernstein polynomials of the equal degree. In the case of the unit commitment problems, the optimization model may be described as a function of the coefficients of the Bernstein polynomials, which is a mixed-integer linear program (MILP). The foundation for continuous time has recently been improved in several aspects. First advantages of continuous time optimization is investigated in marginal pricing in power market industry which leads to following the sub-hourly price deviation leading from exact day-ahead load modeling [37, 38]. The flexible ramp capacity of the generation units is modeled in [39]. In [40] the look-ahead balancing and regulation capacity of the energy storage is modeled by the continuous-time optimization model. Also, the multi-fidelity energy and flexibility reserve co-optimization of the power systems in the day-ahead operation is modeled by the continuous-time optimization using the Bernstein polynomials in [41]. Besides, in order to analyze the flexibility of the power system operation, the continuous-time optimization of the power and the natural gas network is modeled in [42] that helps to model the sub-hourly deviation of the wind generation by modeling the ramp capacity of the flexible resources.

Generally, flexible ramp dispatching models suggested in the technical literature do not specify ramping as an obvious variable; rather, ramping is defined as

the finite difference between discrete power dispatches of resources. In addition, the flexible ramp output is planned using basic discrete-time optimization models with decision intervals that are bigger than the ramping products' binding interval. Consequently, the present discrete-time projections for programming flexible ramp products do not adequately simulate the ramping of resources, which might result in non-deliverable schedules that clash with the energy and reserve plans of producing units.

1.2. Novelties and contributions

According to the reviewed papers, the discreet-time operation of the EDHS has been investigated widely in published works. In the modeled optimization problems, various discrete time intervals have been considered in the proposed mathematical models. For example, 15, 20, 30, and 60 min are the famous time steps modeled in EDHS's optimization models to increase the positive impacts of integrating EDHS. Despite the effectiveness of reducing the time intervals, by increasing the penetration of fluctuating renewable resources, especially wind power producers, the applicability of discrete-time modeling has been questioned. The lack of an appropriate method to use in modeling of electricity and district heating networks to effectively manage the flexibility is required that has not been investigated in literature. Scheduling of electricity and district heating networks has been an important area of study for recent years, which has led to the development of the sophisticated mathematical methods used for this EDHS systems. For example, this is shown by the models used in Danish [43] and Finland [44]. The previous EDHS scheduling models in [23, 45], were based on the usual discrete-time formulation, which implies that time-dependent variables and input parameter have piece-wise constant values. This article focuses on the innovative combination of EDHS scheduling with the continuous-time framework. Specifically, the integrated modeling of continuous-time functioning of complex EDHS cascades presents a number of new issues for EDHS scheduling and continuity constraints. Hence, continuous-time optimization is proposed to effectively model energy systems scheduling in day-ahead

and real-time gates. Nevertheless, continuous-time optimization has not been investigated in modeling the EDHS optimal operation. Also, the impacts of uncertainty on the operation of the EDHS should be considered under the proper uncertainty modeling approach without increasing the computation burden of the optimization problem.

According to the reviewed papers, the main novelties and contributions of this work are as follows:

- A continuous-time model is developed for the operation of the integrated networks of electricity and district heating that improves the flexible operation of the heat and power resources in the sub-hourly markets which has not been investigated in the previous works in the area.
- Continuous-time modeling of the electricity and the district heating network's ramping constraints is modeled in this paper to model the ramping sacristy events in the Barry Island electricity and district heating system.
- Modeling the continuous-time method in the EDHS in the day-ahead and real-time reserve markets for a better performance against the wind generation's uncertainty and system demands.
- Applying the IGDT on modeling the uncertainties in both discrete-time and continuous-time methods of the integrated networks of electricity and district heating and investigating the effectiveness of modeling in the continuous-time and discrete-time optimization according to the opportunities and threats.

The rest of this paper is organized as below. Section 2 represents the discreet time formulation of proposed electricity and district heating network. The continuous-time representation of introduced discreet-time optimization is formulated in section 3. Formulation of IGDT for handling the uncertainty is introduced in section 4. The solutions for mapping the input data into the continuous-time function space and solving methodology of continuous-time

day-ahead and real-time optimization is introduced in section 5. Finally, the paper is concluded in section 6.

2. Continuous-time formulation of the problem

The co-optimization formulation of the energy and day-ahead markets has been previously presented in literature that is a linear hourly optimization problem [31]. Based on the represented model, the day-ahead energy and reserve markets' discrete-time co-optimization is formulated as the following optimization problem. A graphical illustration of the proposed electricity and district heating network is represented in Fig. 1.

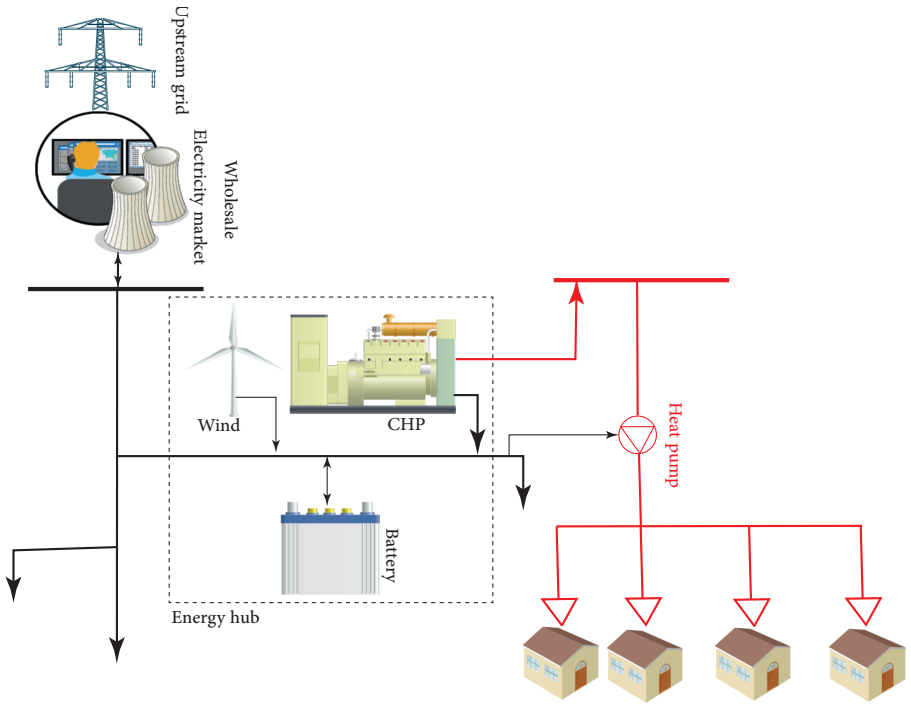

Figure 1: Illustration of proposed electricty and district heating system

2.0.1. Continuous-time electricity and district heating co-dispatch

The following formulation is related to the co-dispatch model of the electricity and district heating network in the day-ahead energy and reserve markets in

the presence of renewable energy sources. The installed capacity of wind power is the biggest in the world, resulting in the greatest variation in power systems. Connecting the electrical and district heating networks is primarily motivated by the variability of wind generation. Thus, in order to avoid complicating the renewable energy system, only the wind power plant is considered in this paper.

$$\sum_{H=h}^{N^{Hub}} \int_{t\in\mathcal{T}} \frac{kC^{NG}(t)}{HV^{NG}} \left(\frac{P_h^{DA,CHP}(t)}{\eta_h^{CHP}} + \mu^{ru} R_h^{ru}(t) + \mu^{rd} R_h^{rd}(t) \right) dt \tag{1}$$

$$P_h^{DA,CHP}(t) + R_h^{ru}(t) \leqslant \overline{P}_h(t) \tag{2}$$

$$P_h^{DA,CHP}(t) - R_h^{rd}(t) \geqslant \underline{P}_h(t) \tag{3}$$

$$\dot{P}^{DA,CHP}(t) + \dot{R}^{Up}(t) - \dot{R}^{Dn}(t) \leqslant \overline{\dot{P}}(t) \tag{4}$$

$$\dot{P}^{DA,CHP}(t) + \dot{R}^{Up}(t) - \dot{R}^{Dn}(t) \geqslant -\overline{\dot{P}}(t) \tag{5}$$

$$P^{DA,CHP}(t) + P^{WND}(t) = P^{EH}(t) + P^{HP}(t) \tag{6}$$

$$P_j^G(t) + P_{i,j}(t) = \sum_{k\in S_j^{B,d}} P_{j,k}(t) + P_j^L(t) \tag{7}$$

$$P_h^{DA,CHP}(t)(1 - \eta_h^{CHP} - \eta_h^{CHP,L})/\eta_h^{CHP} + P_h^{HP}(t)\, COP_h^{HP} = H_h^{EH}(t) \tag{8}$$

$$Q_j^G(t) + Q_{i,j}(t) = \sum_{k\in S_j^{B,d}} Q_{j,k}(t) + Q_j^L(t) \tag{9}$$

$$V_{i,j}(t) = V_i(t) - (P_{i,j}(t) r_{i,j} + Q_{i,j}(t) x_{i,j})/V_0 \tag{10}$$

$$H_n^S(t) = C^P m_n^S(t)(T_n^S(t) - T_n^R(t)) \tag{11}$$

$$H_n^L(t) = C^P m_m^L(t)(T_n^S(t) - T_n^R(t)) \tag{12}$$

$$T_p^{out}(t) = (T_p^{in}(t) - T_p^{Amb}(t))e^{-\frac{\lambda_p L_p}{C^P m_p(t)}} + T^{Amb}(t) \tag{13}$$

$$\sum_{p \in S_n^{P,h}} (m_p(t) T_p^{out}(t)) = \sum_{pi \in S^{P,h}} (m_p(t)) T_n^{mix}(t) \tag{14}$$

$$T_p^{in}(t) = T_n^{mix}(t) \quad \forall p \in S^{P,s} \tag{15}$$

In the above formulation:

$$\dot{P}_h^{DA,CHP}(t) = \frac{dG_h^{DA,CHP}(t)}{dt} \tag{16}$$

$$\dot{R}_h^{ru}(t) = \frac{dR_h^{ru,CHP}(t)}{dt} \tag{17}$$

$$\dot{R}_h^{rd}(t) = \frac{dR_h^{rd,CHP}(t)}{dt} \tag{18}$$

The aforementioned formulation represents the continuous-time operation of the electricity and district heating networks in the day-ahead energy and reserve markets. The energy storage units along with the heat pumps are utilized to cover the variations of wind generation, electricity, and heat demand on a real-time scale due to their flexible nature. The first term of the objective function represents the operation cost in the day-ahead market, while the reserve market cost is included in the second to the fourth terms for the generation units and storage devices. The minimum and maximum generation power of CHP units in the day-ahead and real-time markets is limited by the constraints (2) and (3). Besides, the ramp-up and ramp-down limits of the generation units are restricted through constraints (4) and (5). The power balance equation of the energy hubs is represented in (6). Also, the active power balance of the network is also determined in (7). The heat balance equation of the energy hubs is

represented in (8). Besides, the reactive power balance of the network is illustrated in (9). In this paper, the electricity network has a radial topology [46]. The formulation of the linear power flow is coordinated with the district heating network heat flow. The linear approximation of the AC power flow methods is represented in (10) [47, 48]. Noted that the mentioned linear power flow equation is derivable by the specific assumptions on the voltage and power angles introduced in [49]. The incorporation of the voltage and reactive power are the advantages of the considered power flow more than the well-known DC flow. The district heating networks, based on their control strategies, are divided into four categories, including variable flow and variable temperature, variable flow and constant temperature, constant flow and variable temperature, constant flow, and constant temperature. In this paper, the constant flow and variable temperature are considered as the control strategy of the district heating network that the equations are represented in (11)-(15) [49]. Equations (11) and (12) represent the supplied and consumed heat power in the hub and load nodes, respectively. Equation (13) represents the drop of temperature along the network pipelines which is similar to the supply and return pipelines. The district heating network nodes' temperature is known as the mixture temperatures that could be evaluated for the confluence nodes by (14). Equation (15) ensures the mas flows that are leaving from the same temperature confluence node.

2.0.2. Continuous-time modeling of energy storage

The energy storage can be operated in both energy arbitrage and regulation reserve modes to gain more income. Purchasing energy at low price times and selling it at high price times is a well-known strategy for energy arbitrage of energy storage systems. In this paper, this property is neglected due to the non-market environment. Also, the energy storage is scheduled in the day-ahead market to reduce the scarcity events of the generation units. This study aims to use the stored energy as the regulation reserve to deal with the uncertainties. By neglecting the energy arbitrage of energy storage systems, the formulation of the energy storage device in the continuous-time method could be represented

as below to participate in the regulation market:

$$Min \int_{t\in\mathcal{T}} \left(q_r^{reg}\delta^{ru}(t) + q_r^{reg}\delta^{rd}(t)\right) dt \tag{19}$$

$$\int_{t_d-1}^{t_d} \frac{dE_r(t)}{dt} = \int_{t_d-1}^{t_d} \left(\eta^{ch} d_r(t) - \frac{g_r(t)}{\eta^{dch}}\right) \tag{20}$$

$$d_r = q^{reg}\,\delta^{ru}(t) + d_r^{DA}(t) \tag{21}$$

$$g_r = q^{reg}\,\delta^{rd}(t) + g_r^{DA}(t) \tag{22}$$

$$0 \leqslant d_r(t) \leqslant \bar{d}_r \tag{23}$$

$$0 \leqslant g_r(t) \leqslant \bar{g}_r \tag{24}$$

$$\underline{E}_r \leqslant E_r(t) \leqslant \bar{E}_r \tag{25}$$

$$\underline{\dot{d}}_r \leqslant \frac{d(d_r(t))}{dt} = \dot{d}_r(t) \leqslant \bar{\dot{d}}_r \tag{26}$$

$$\underline{\dot{g}}_r \leqslant \frac{d(g_r(t))}{dt} = \dot{g}_r(t) \leqslant \bar{\dot{g}}_r \tag{27}$$

The payment of the system to the storage units in the regulation markets can be evaluated by using the continuous-time equation (19). Besides, the continuous-time differential equation (20) is used to control the state of energy in the storage units during the whole scheduling period. In addition to the regulation market, Equations (21) and (22) indicate the energy storage that can be scheduled in the day-ahead market in the energy arbitrage model. Moreover, the minimum and maximum limits of the charging/discharging power and energy state of the energy storage are limited by the constraints (23)-(25), respectively. Also, the charging and discharging ramp limits of the energy storage are limited by differential constraints (26) and (27).

3. Modeling continuous-time equations in Bernstein function space

Various approaches and function spaces are proposed in different studies to model the continuous-time problems in the optimization programming [42]. In this paper, the Bernstein polynomial is selected to model a set of discreet

data as the continuous-time programming problem in the finite-order function space. The proposed finite-order function space is the Bernstein function space that is spanned by the Bernstein polynomial approach. The main reason for selecting the Bernstein polynomial is the smooth movement, not only in the breakpoints but also between two breakpoints. More details for selecting the Bernstein polynomials are represented as follows:

3.1. Bernstein polynomials approach

Assuming that the Bernstein polynomials degree Q is used to model the discreet spaces between the time intervals, the $Q+1$ number of Bernstein basis polynomials should be defined by using the following equation:

$$e^{t}_{q,Q} = \binom{Q}{q} t^{q}(1-t)^{Q-q} \tag{28}$$

In (28) the phrase $\binom{Q}{q}$ shows a binomial coefficient. For example, for continuous-time modeling the function $x(t)$ in the time interval $\mathcal{T}$, first the mentioned time interval $\mathcal{T}$ should be divided into D intervals as $\mathcal{T} = [t_d, t_{d+1})$ in which $\mathcal{T} = \cup_{d=1}^{D} \mathcal{T}_d$; thus the length of separate interval is $\mathcal{T} = t_{d+1} - t_d$. As illustrated in Fig. 2, the intervals are formed by a set of basis functions, that are functions of Bernstein polynomials of degree Q, multiplied by the Bernstein coefficients. Finally the Bernstein polynomial operator $\Phi^{x(t)}_{Q_d}$ is used to map the continues function $x(t)$ in the Bernstein function space in (29).

$$\Phi^{x(t)}_{Q_d} = \sum_{q_d}^{Q_d} B^{x(t)}_{q_d} e^{t-t_d}_{q_d,Qd} \ , \quad t \in [t_d, t_{d+1}) \tag{29}$$

where the parameter $B^{x(t)}_{q_d}$ is the control point of the Bernstein polynomial in the function space that known as the Bernstein coefficient. In addition to the mentioned properties of the Bernstein polynomials, some other advantages makes this function space more attractive to model the problem. Firstly, it is

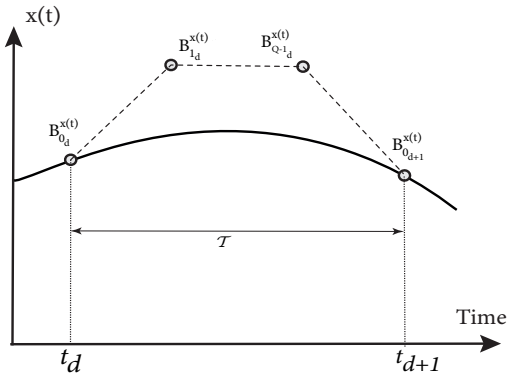

Figure 2: Coefficients of Bernstein polynomials

necessary to reduce the approximation error by increasing the degree of Q in the $\Phi^{x(t)}_{Q_d}$. In other words:

$$\lim_{Q_d \to \infty} \Phi^{x(t)}_{Q_d} = x(t) \tag{30}$$

Secondly, the derivation property of the Bernstein polynomials, i.e., the derivative of $\Phi^{x(t)}_{Q_d}$ is equivalent with the deviation of the two lower degree polynomials as indicated in (31).

$$\frac{d\,\Phi^{x(t)}_{Q_d}}{dt} = Q \sum_{q_d=0}^{(Q-1)_d} (B^{x(t)}_{q_d} - B^{x(t)}_{(q-1)_d}) e^t_{q_d,(Q-1)_d} \tag{31}$$

The third state is obtained from the convex hull property of basis functions that leads to that the Bernstein coefficients of the $\Phi^{x(t)}_{Q_d}$ and $\dot{\Phi}^{x(t)}_{(Q_d-1)}$ are bounded in their minimum and maximum limits that is indicated in (32).

$$\min\{B^{x(t)}_{q_d}\} \leqslant \vec{B}^{x(t)}_{q_d} \leqslant \max\{B^{x(t)}_{q_d} \tag{32}$$

Finally, the fourth state is the continuity of the function between the last point of the previous interval with the first point of the present interval that enforces by definition of the following two constraints that are known as the continuity conditions.

$$B^{x(t)}_{0_d} = B^{x(t)}_{Q_{d-1}} \tag{33}$$

$$B^{x(t)}_{1_d} - B^{x(t)}_{0_d} = B^{x(t)}_{Q_{(d-1)}} - B^{x(t)}_{(Q-1)_{d-1}} \tag{34}$$

The mentioned two constraints (33) and (34) are important to maintain the continuity of the generation and ramping trajectories at the time of transmission between time intervals. The last property is the integral operator on the Bernstein polynomials that would be useful in the computation of the objective function. This property can be stated as below:

$$\int_{t_d}^{t_{d+1}} \Phi^{x(t)}_{Q_d} = \int_{t_d}^{t_{d+1}} (\vec{B}^{x(t)}_{Q_d}\, \vec{e}^{t}_{Q_d})dt = \vec{B}^{x(t)}_{Q_d} \int_{t_d}^{t_{d+1}} \vec{e}^{t}_{Q_d}\, dt = \frac{\vec{B}^{x(t)}_{Q_d}.\mathbf{1}_{Q_d}}{Q_d+1} = \frac{\sum_{q_d=0}^{Q_d} \vec{B}^{x(t)}_{q_d,Q_d}}{Q_d+1} \tag{35}$$

3.2. Modeling the problem in the Bernstein function space

The proposed continuous-time optimization problem (1) and (27), is computationally intractable because it has a infinite-dimensional decision space. Therefore, in this section a solution method based on the function space is proposed to solve the proposed infinite-dimensional continuous-time optimization problem (1) and (27). The proposed function space-based method reduces the dimensionality of the continuous-time trajectories. In other words, the proposed function space-based method seeks to model the the continuous-time trajectories in the finite-order function space that in this paper the Bernstein polynomials is chosen for this propose.

3.2.1. Objective function

Based on the stated context of this section, by substituting the variables of the continuous-time modeling, the objective functions (1) and (19) can be represented in the infinite-dimensional Bernstein function space that is represented in (36). Moreover, based on the introduced Bernstein polynomials' integral property in this section, by integrating the infinite dimensional equation (36) over T, the linear and finite-dimensional cost function of the CHP units and storage units in the day-ahead and real-time market is represented in (37). The first term of the objective function (37),is related to the day-ahead operation

cost of the CHP units. The regulation up and down cost of the CHP units are represented in the second and third term of objective function (37). Also, the fourth and fifth terms of (37) model the regulation up and down cost of the energy storage devices.

$$\overbrace{\left(\sum_{h=1}^{H}\left(\int_{t\in\mathcal{T}}\frac{k\,C^{NG}(t)}{HV^{NG}}\times\left[\vec{B}_{Q_d}^{G_{h,t}^{DA,CHP}}\vec{e}_{Q_d}^{t}+\mu^{ru,CHP}\vec{B}_{Q_d}^{R_{h,t}^{ru,CHP}}\vec{e}_{Q_d}^{t}+\mu^{rd,CHP}\vec{B}_{Q_d}^{R_{h,t}^{ru,CHP}}\vec{e}_{Q_d}^{t}\right]dt\right)+\sum_{r=1}^{R}\left(\int_{t\in\mathcal{T}}\left[\mu^{ru,S}q_r^{res}\vec{B}_{Q_d}^{R_{r,t}^{ru,S}}\vec{e}_{Q_d}^{t}+\mu^{rd,S}q_r^{res}\vec{B}_{Q_d}^{\delta_{r,t}^{rd,S}}\vec{e}_{Q_d}^{t}\right]dt\right)\right)}^{Minimize} \tag{36}$$

$$\overbrace{\left(\sum_{h=1}^{H}\sum_{t=1}^{T}\frac{k\,C^{NG}(t)}{HV^{NG}}\times\sum_{d}^{D}\frac{\sum_{q_m}^{Q}\left[B_{q_d,Q_d}^{G_{h,t}^{DA,CHP}}+\mu^{ru,CHP}B_{q_d,Q_d}^{R_{h,t}^{ru,CHP}}+\mu^{rd,CHP}B_{q_d,Q_d}^{R_{h,t}^{ru,CHP}}\right]}{Q_d+1}+\sum_{r=1}^{R}\sum_{t=1}^{T}\sum_{d}^{D}\frac{\sum_{q_m}^{Q}\left[\mu^{ru,S}q_r^{res}B_{q_d,Q_d}^{R_{r,t}^{ru,S}}+\mu^{rd,S}q_r^{res}B_{q_d,Q_d}^{\delta_{r,t}^{rd,S}}\right]}{Q_d+1}\right)}^{Minimize} \tag{37}$$

3.2.2. Electric and heat loads and wind generation profiles

In this section, the Bernstein representation of the electric and heat loads and wind power is formed to use in the model. By modeling the electric and non-electric loads, and wind generation in the Bernstein function space, the following vectors in the form of the Q-degree Bernstein basis functions with the length of d for each time interval can be defined.

$$\begin{cases}\Phi_{Q_d}^{\Theta}=\vec{B}_{Q_d}^{\Theta}e_{Q_d}^{t-t_d}\\ \forall t\in[t_d,t_{d+1}),\Theta\in\{P_j^L(t),H_n^L(t),P_h^{RES}(t)\}\end{cases} \tag{38}$$

In the mentioned equation (38), $\vec{B}_{Q_d}$ represents the Bernstein coefficient of the parameter that comes from the values of parameters.

3.2.3. power and district heating network constraints

In this sub-section, the Bernstein representation of the infinite order continuous-time constraints introduced in the previous section is represented in the form of the linear formulation.

$$lB_{Q_d}^{G_h^{DA,CHP}(t)} + B_{Q_d}^{R_h^{up}(t)} < \bar{G}_h \tag{39}$$

$$lB_{Q_d}^{G_h^{DA,CHP}(t)} - B_{Q_d}^{R_h^{dn}(t)} < \underline{G}_h \tag{40}$$

$$\left(B_{Q_d}^{G_h^{DA,CHP}(t)} - B_{(Q_d-1)}^{G_h^{DA,CHP}(t)}\right) + \left(B_{Q_d}^{R_h^{up}(t)} - B_{(Q_d-1)}^{R_h^{up}(t)}\right) - \left(B_{Q_d}^{R_h^{dn}(t)} - B_{(Q_d-1)}^{R_h^{dn}(t)}\right) \leqslant \frac{\bar{\dot{G}}}{Q_d} \tag{41}$$

$$\left(B_{Q_d}^{G_h^{DA,CHP}(t)} - B_{(Q_d-1)}^{G_h^{DA,CHP}(t)}\right) + \left(B_{Q_d}^{R_h^{up}(t)} - B_{(Q_d-1)}^{R_h^{up}(t)}\right) - \left(B_{Q_d}^{R_h^{dn}(t)} - B_{(Q_d-1)}^{R_h^{dn}(t)}\right) \geqslant \frac{\underline{\dot{G}}}{Q_d} \tag{42}$$

$$B_{Q_d}^{G_h^{DA,CHP}(t)} + B_{Q_d}^{P_h^{RES}(t)} = B_{Q_d}^{P_h^{EH}(t)} + B_{Q_d}^{P_h^{HP}(t)} \tag{43}$$

$$B_{Q_d}^{P_h^{DA,CHP}(t)}(1 - \eta_h^{CHP} - \eta_h^{CHP,L})/\eta_h^{CHP} + B_{Q_d}^{P_h^{HP}(t)} COP_h^{HP} = H_h^{EH}(t) \tag{44}$$

$$B_{Q_d}^{P_j^G(t)} + B_{Q_d}^{P_{ij}(t)} = \sum_{k \in S_j^{B,x}} B_{Q_d}^{P_{ik}(t)} + B_{Q_d}^{P_j^L(t)} \tag{45}$$

$$B_{Q_d}^{QP_j^G(t)} + B_{Q_d}^{QP_{ij}(t)} = \sum_{k \in S_j^{B,x}} B_{Q_d}^{QP_{ik}(t)} + B_{Q_d}^{QP_j^L(t)} \tag{46}$$

$$B_{Q_d}^{V_j(t)} = B_{Q_d}^{V_i(t)} - (B_{Q_d}^{P_{jj}(t)} rr_{i,j} + B_{Q_d}^{QP_{jj}(t)} xr_{i,j})/V_0 \tag{47}$$

$$B_{Q_d}^{H_n^S(t)} = C^P B_{Q_d}^{m_n^S(t)} (B_{Q_d}^{T_n^S(t)} - B_{Q_d}^{T_n^R(t)}) \tag{48}$$

$$B_{Q_d}^{H_n^L(t)} = C^P B_{Q_d}^{m_n^L(t)} (B_{Q_d}^{T_n^S(t)} - B_{Q_d}^{T_n^R(t)}) \tag{49}$$

$$B_{Q_d}^{T_p^{out}(t)} = (B_{Q_d}^{T_p^{in}(t)} - T_t^A) e^{-\frac{\lambda_p L_p}{C^P B_{Q_m}^{m_p(t)}}} + T^A \tag{50}$$

$$\sum_{S_n^{P,h}} (B_{Q_d}^{m_p(t)} B_{Q_d}^{T_p^{out}(t)}) = \sum_{S_n^{P,h}} (B_{Q_d}^{m_p(t)}) B_{Q_d}^{T_p^{mix}(t)} \tag{51}$$

$$B_{Q_d}^{T_p^{in}(t)} = B_{Q_d}^{T_p^{mix}(t)} \qquad \forall p \in S_n^{t,h} \tag{52}$$

The above formulation represent the continuous-time form of the formulation (1)-(18). In the continuous-time formulation, the decision variables are the Bernstein coefficient that is modeled in the formulation (1)-(18). For example,

the Bernstein coefficients of variable $G_h^{DA,CHP}(t)$ is the vector $B_{Q_d}^{G_h^{DA,CHP}(t)}$ that is used in constraint (39). The constraint (39) and (40) represent the minimum and maximum amounts of generation trajectories that are the continuous-time model of (2) and (3). Also, the continuous-time ramping trajectories of the continuous-time modeling is limited by the (41) and (42). Other continuous-time constraints (43)-(52) are the continuous-time representation of the discreet time formulation stated in (2)-(15). The other main difference between the discreet time and continuous-time modeling is the continuity constraints on the variables over the first and endpoints of the time intervals that should be defined as below.

$$\begin{cases} B_{0_d}^{\Psi} = B_{Q_{d-1}}^{\Psi} \\ B_{1_d}^{\Psi} - B_{0_d}^{\Psi} = B_{Q_{d-1}}^{\Psi} - B_{(Q-1)_{d-1}}^{\Psi} \end{cases} \tag{53}$$

The mentioned continuity conditions (53) are considered for the following variables set.

$$\Psi \in \{G_h^{DA,CHP}(t), R_h^{up}(t), R_h^{dn}(t), V_i(t), T_n^R(t), T_n^T(t)\}$$

3.2.4. Energy storage model

The Bernstein function space representation of the energy storage devices model (19)-(27) is represented in this section. The operation cost of storage in the reserve market is included in the objective function (37) that has been refrained the re-expressing the Bernstein function space representation of storage cost function (19). The constraints (20)-(27) respectively can be represented in the function space as below.

$$B_{(Q+1)_d}^{E_r(t)} - B_{(Q+1)_d}^{E_r(0)} = \eta^{ch} B_{Q_d+1}^{d_r(t)} - \frac{B_{Q_d+1}^{g_r(t)}}{\eta^{dch}} \tag{54}$$

$$B_{Q_d}^{d_r(t)} = q^{reg} B_{Q_d}^{\delta_r^{ru}(t)} + B_{Q_d}^{d_r^{DA}(t)} \tag{55}$$

$$B_{Q_d}^{g_r(t)} = q^{reg} B_{Q_d}^{\delta_r^d(t)} + B_{Q_d}^{g_r^{DA}(t)} \tag{56}$$

$$0 \leqslant B_{Q_d}^{d_r(t)} \leqslant \bar{d}_r \tag{57}$$

$$0 \leqslant B_{Q_d}^{g_r(t)} \leqslant \bar{g}_r \tag{58}$$

$$\underset{-r}{E} \leqslant B_{Q+1}^{E_r(t)} \leqslant \bar{E}_r \tag{59}$$

$$\frac{\dot{d}}{\underset{-r}{Q_d}} \leqslant \left(B_{Q_d-1}^{d_r(t)} - B_{Q_d}^{d_r(t)}\right) \leqslant \frac{\bar{\dot{d}}_r}{Q_d} \tag{60}$$

$$\frac{\dot{g_r}}{\underset{-}{Q_d}} \leqslant \left(B_{Q_d-1}^{g_r(t)} - B_{Q_d}^{d_r(t)}\right) \leqslant \frac{\bar{\dot{g}}_r}{Q_d} \tag{61}$$

4. Information gap decision theory

The IGDT is a classical risk assessment method that is used to evaluate the effects of the uncertain parameters. The IGDT uses the two functions to obtain the robustness and opportunity strategies in the optimization problem. The opportunity function considers the good realizations of the uncertain parameters on improving the objective function. In contrast, the robustness function tries to model the threats imposing from the uncertain parameters on the objective function. More details of the IGDT is available in [50]. The mathematical formulation of the IGDT is represented below.

$$\max \ \pm\varphi \tag{62}$$

$$P^{RES}(t) = (1 \mp \varphi).\bar{P}^{RES}(t) \tag{63}$$

$$\vartheta \leqslant \overbrace{\vartheta_b(1 \pm \alpha)}^{\Omega}, \Omega \in \{RO, OP\} \tag{64}$$

In the formulation (62)-(64), $-$ and $+$ determine the robustness (RO) and opportunity (OP) strategies. Also, ϑ_b refers to the base cost of the base optimization problem, and α deviates the cost from the base value upward or downward based on the considered risk strategy. For example, in the robustness strategy, $-$ is considered, and the φ is maximized while the total cost is less than $\vartheta_b(1-\alpha)$ that is downward of the base cost ϑ_b.

5. solution methodology

The used load and renewable data in day-ahead scheduling are mostly discrete hourly data. Because of the definition of continuity constraints on most variables in the continuous-time modeling, projecting the input load and wind data into the continuous-time function space is critical in obtaining a continuous-time generation and scheduling. We now want to expand cubic splines on two well-known bases: the cubic Hermite basis and Bernstein polynomials of degree 3. The cubic Hermite basis enables us to specify the expansion coefficients as generation samples and their changing rate, i.e., the ramp. The Bernstein polynomials may be used as a proxy expansion to impose limits on maximum capacity and ramping of the modeled continuous-time generation with an equal number of coefficients. Let us begin by modeling the hourly day-ahead load and wind profile using cubic Hermite splines. Instead of sampling uniformly, we expand the model and use arbitrary endpoints to divide the day-ahead programming horizon into equal intervals $0, t_1, t_2, t_3, ...$ In [51], the four cubic Hermite polynomial bases are used for $t \in [0, 1)$ as follows:

$$X_{00}(t) = (2t^3 - 3t^2 + 1)\, H_{00}(t) \tag{65}$$

$$X_{01}(t) = (t^3 - 2t^2 + 1)\, H_{01}(t) \tag{66}$$

$$X_{10}(t) = (-2t^2 + 3t^2)\, H_{10}(t) \tag{67}$$

$$X_{11}(t) = (t^3 - t^2)\, H_{11}(t) \tag{68}$$

The H represents the Hermit coefficients. Thus, the cubic Hermite approximation of the day-ahead wind and load profile can be expressed as:

$$X(t) = \sum_{m=0}^{M-1} H(\tau_m)\, e_m^H(t) \tag{69}$$

The introduced optimization problem of electricity and district heating network is in the Bernstein function space. Thus, defining the mapped load and wind Hermit basis in the Bernstein function space is required for solving the optimization problem in the Bernstein function space. For converting the Hermit coefficients to the Bernstein coefficient, the similarity of the two coefficients should be investigated. The coefficients of the cubic Hermit function are represented in Fig. 3.

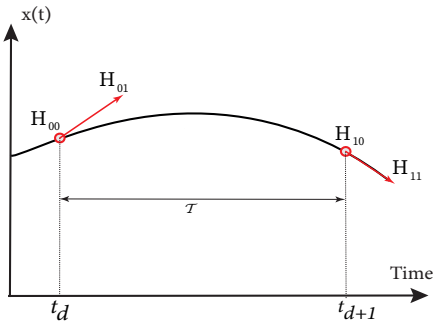

Figure 3: Coefficients of Hermit polynomials

As shown in Fig. 3, the cubic Hermite load approximation coefficients are specified only by the load value and its derivative at the interval's beginning and ending points. According to , there is a linear mapping between the Bernstein and Hermit basis of degree 3, which could be defined as below:

$$\mathbf{H(t)} = \mathbf{W}\,\mathbf{B_3(t)} \tag{70}$$

Where the basis's change matrix $\mathbf{W}$can be defined as below:

$$\mathbf{W} = \begin{pmatrix} 1 & 1 & 0 & 0 \\ 0 & {}^{1}/_{3} & 0 & 0 \\ 0 & 0 & 1 & 1 \\ 0 & 0 & {}^{-1}/_{3} & 0 \end{pmatrix} \tag{71}$$

Therefore, the defined Hermit polynomial can be modeled in the Benstein func-

tion space as below.

$$X(t) = \sum_{m=0}^{M-1} B_3^T(\tau_m) W^T e_m^H = \sum_{m=0}^{M-1} B_3^T(\tau_m) e_m^B \tag{72}$$

Using the above mentioned method, the Benstein equivalent of Hermit basis will be obtained to use in the optimization procedure.

5.1. Continuous-time optimization procedure

This paper proposes a continuous-time optimization procedure for the coordinated operation of electricity and district heating networks to solve the day-ahead and real-time operation problem. As mentioned, the continuous-time optimization problem needs to project all decision variables and parameters to a continuous-time function space, which the Bernstein function space is proposed in this paper. Due to direct connectivity with real data, the Hermit function is used as a tool to transform the real data into Bernstein coefficients. The procedure of the proposed continuous-time optimization is represented in Fig.4. In addition to the deterministic optimization represented above, the IGDT-based optimization procedure of the proposed continuous-time problem could be calculated using the algorithm represented in Fig. 5.

6. CASE STUDIES

In order to show the effectiveness of the proposed continuous-time framework, the Barry Island system is proposed in this paper, and the schematic diagram is illustrated in Fig. 2. The mentioned test system is composed of a 9-bus power distribution network and a 32-node district heating network [49] that three energy hubs connected to buses 1, 6, 9 to supply all electricity and heat loads existing in the system. Energy hubs 1 and 3 consists of one CHP unit to provide the heat and electricity loads and one heat pump to supply the heat loads. In addition to the mentioned units, the wind farm and energy storage system are installed in the energy hub 2. The economical and technical characteristics of the used units in the model and are available in [49].

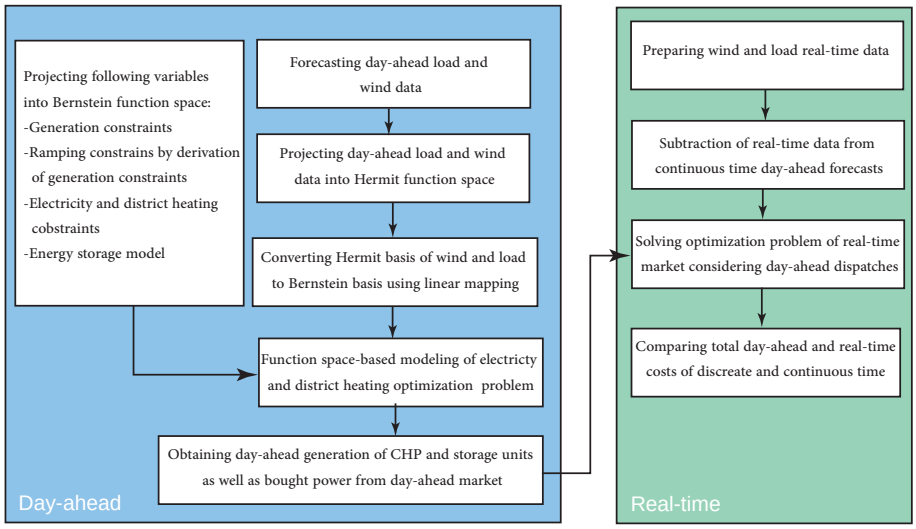

Figure 4: Continuous-time Optimization procedure

The main input parameters are the wind power generation of the wind farm that is installed in the energy hub 2 and the system's heat and power loads. The proposed system's load data is derived from the California ISO (CAISO) for August 12, 2019, that the day-ahead and real-time information is scaled down to 1.6 MW to form the load trajectories of the proposed model. Moreover, the wind generation trajectories are also derived from the CAISO and scaled down to 500 kw to use in the proposed system. The continuous-time day-ahead, discrete-time day-ahead, and real-time values of the power and heat load and wind generation power are used in the proposed model, and it is determined in Fig. 3. The discrete-time results are obtained by solving the 24-hour discrete-time optimization problem in the day-ahead market. Besides, The 20 min (72 intervals) discrete-time optimization problem is used in the discrete-time reserve operation. Similarly, the Bernstein function space degree 3 is used to model the continuous-time day-ahead and reserve operation.

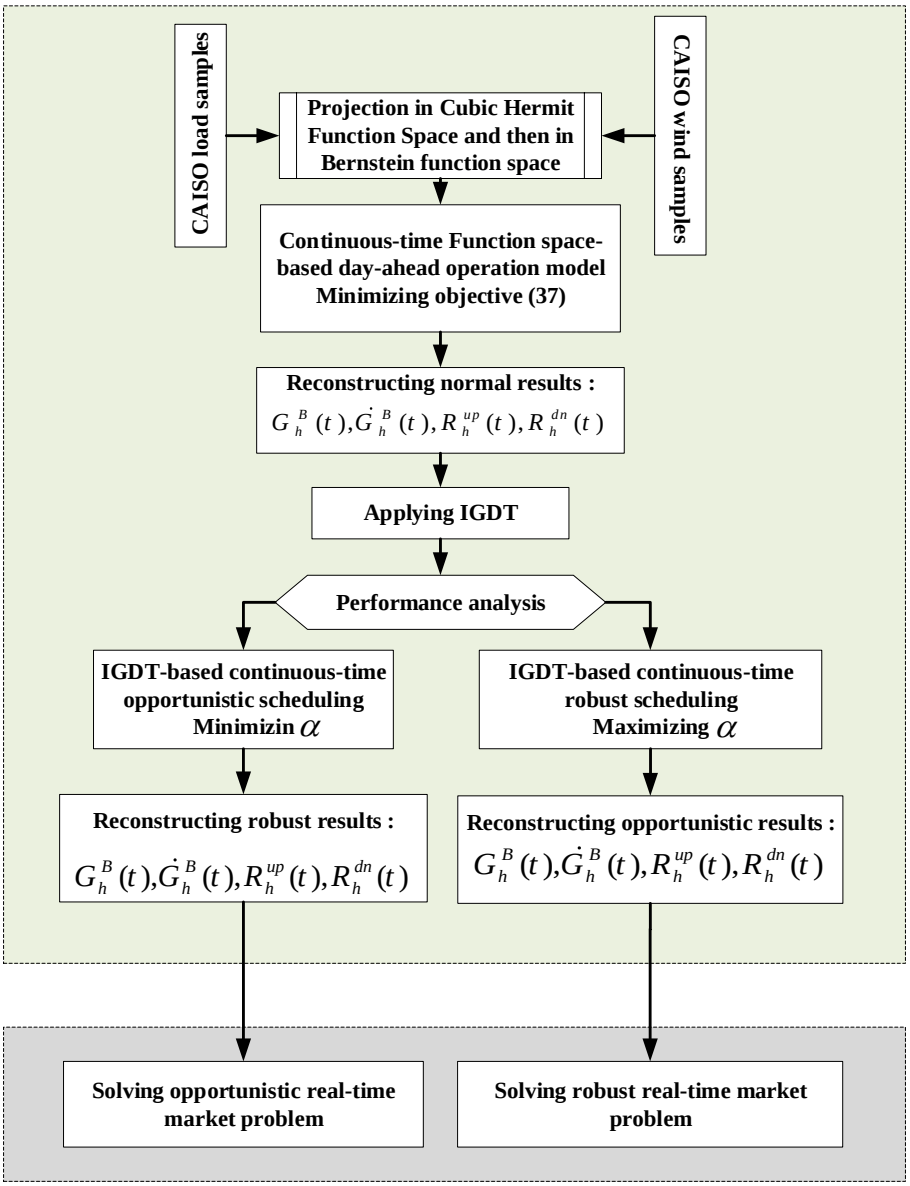

Figure 5: IGDT-based solving algorithm of the model

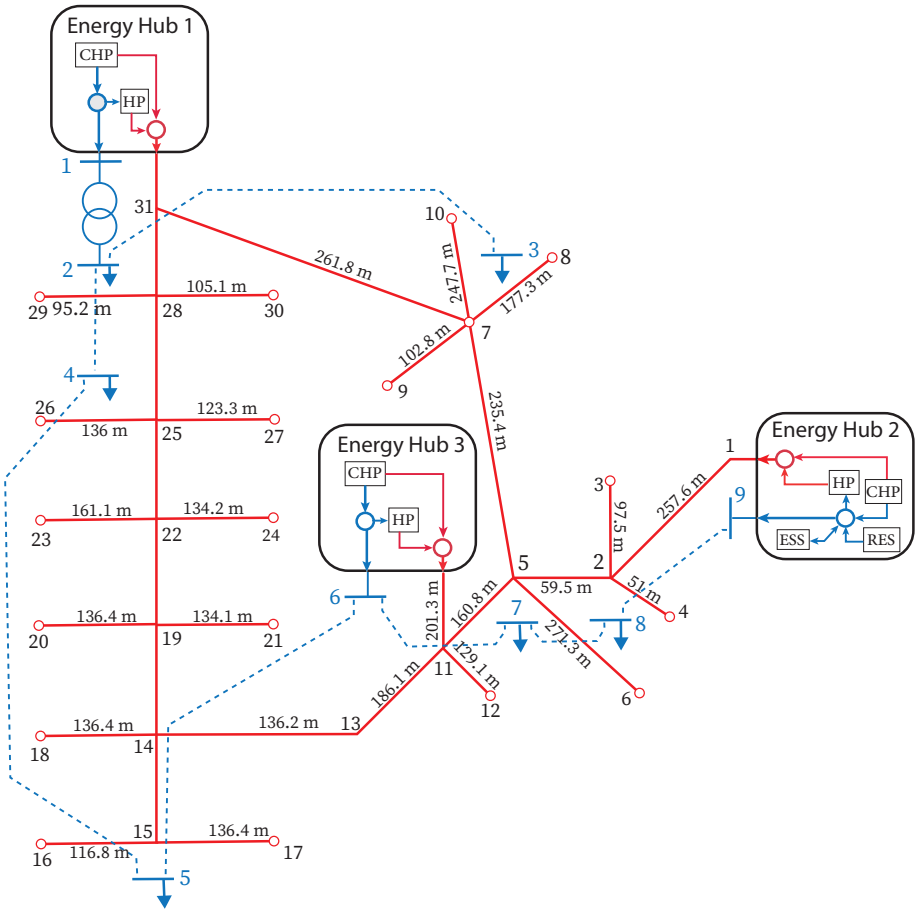

Figure 6: Schematic diagram of the Barry Island system

6.1. Numerical results

6.1.1. Day-ahead and real-time reserve operation cost

The EDHS operation costs in the two continuous-time and discrete-time modeling methods are represented in Table 1. The Continuous-time operation could lead to higher cost in day-ahead scheduling which must be compensated in the next gates (like reserve market) to be justified. Therefore, to show the advantage of the proposed method, day-ahead and reserve costs are selected for calculation as shown in Table 1. The day-ahead cost of both discrete-time and continuous-time models are related to the day-ahead operation of CHP, and

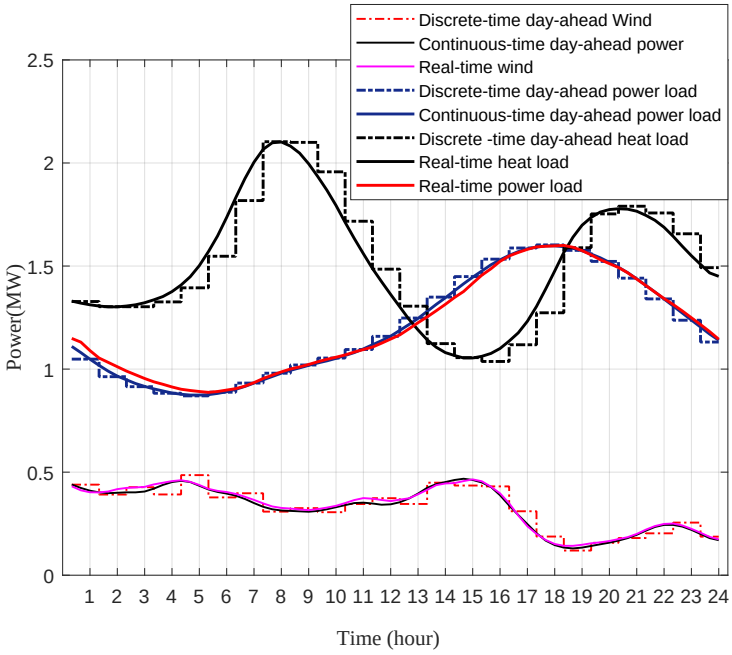

Figure 7: Input parameters of the discrete-time and continuous-time models

storage units that are reflected in (37). Besides, the reserve cost is related to the both up and down reserves provided by the storage and CHP units. The main advantage of the continuous-time modeling approach manifested in the total operation cost that is less than the discrete-time model by 0.91%. Based on Table 1 the EDHS operation cost in the day-ahead market are \$961 and \$942 for the continuous-time and discrete-time models, respectively. The higher operation cost of continuous-time model in the day-ahead market is compensated in the real-time reserve market so that operation costs become \$23 and \$51 for the continuous-time and discrete-time models, respectively. The reason for this cost reduction is due to fewer requirements for high ramping in the real-time market. The generated power by power and heat generation units has lower cost compared to the the energy storage devices. At the real-time market, the available power of power and heat generating units has priority to provide the required ramp. If the provided ramping through the power and district heating

network is not enough for supplying the required ramp, the ramping provided by energy storage devices will be used to eliminate the ramping scarcity events. Thus, having a large district heating network will be help in reducing the overall cost of the integrated electricity and district heating networks

Table 1: Comparison of operation costs in the continuous-time and discrete-time modelings

	Day-ahead cost ($)	Real-time reserve cost ($)	Total cost ($)
Discrete-time	942	51	993
Continuous-time	961	23	984

6.1.2. Day-ahead operation of EDHS components

The continuous-time and discrete-time operation of the HP and CHP units is represented in Fig. 8. Furthermore, the level of energy in the ES that is determined by the day-ahead and real-time reserve operation is illustrated in Fig. 9. The main reason for the lower operation cost in the day-ahead operation of the discrete-time method compared to continuous-time model and the consequences are illustrated in Figs. 8 and 9. Based on Fig. 8 it can be shown that in the day-ahead operation of the discrete-time model, the generated power of the HP and CHP units is constant, while in the continuous-time model, the operation of the units smoothly changes over time. Moreover, the HP system's ramp capacity is considerable, which is a positive aspect of the heat loads supplying process. The fixed hourly day-ahead operation of the discrete-time model leads to more flexible resources in the reserve market that will be demonstrated in the following results.

The continuous-time energy trajectories and discrete-time hourly operation of the energy storage are determined in Fig. 9. As Fig. 9 illustrates, the discrete-time operation of the energy storage device is more than the continuous-time model due to the more required flexibility of the discrete-time method in the reserve market that will be represented. Frequent usage of the energy storage in the reserve market of the discrete-time model is one of the higher costs of

the method in the reserve market. The reason for more usage of energy storage in reserve market is related to the ramping scarcity of power generation units which causes the energy storage to provide more flexible ramp in reserve market. Also, Fig. 9 show that the slope of the charging and discharging energy in the discrete-time model is higher than the continuous-time model. Supplying these high rate charging and discharging ramps in the regulation markets is high-costly for system operators.

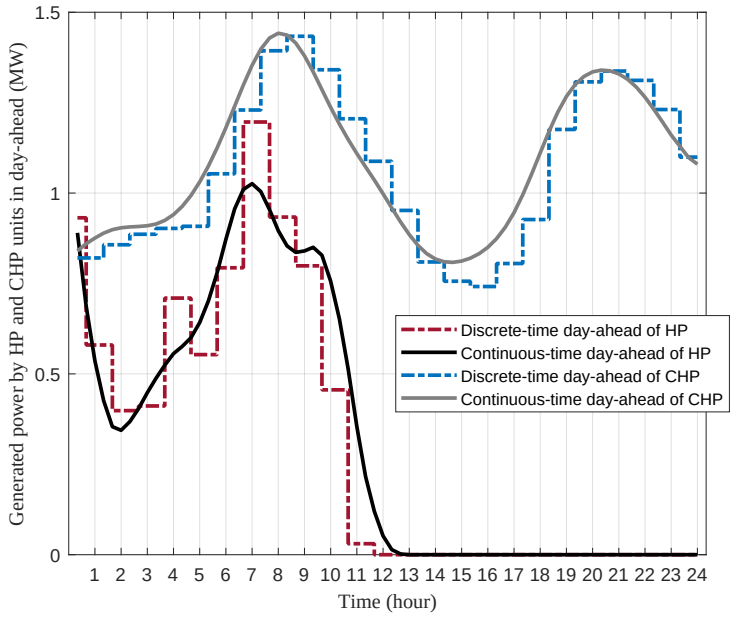

Figure 8: Generated power by HPs and CHPs

6.1.3. Requirement of power in the real-time reserve market

As mentioned earlier, the reserve cost of the discrete-time optimization model is more than the continuous-time model. The reason for this higher cost is depicted in Fig. Significant load variation and several rapid ramping occurrences contribute to the comparatively high real-time operating cost. 10. The short-term operation in the real-time reserve market along with the effects of the hourly spikes in the hourly day-ahead operation leads to severe jumps in the

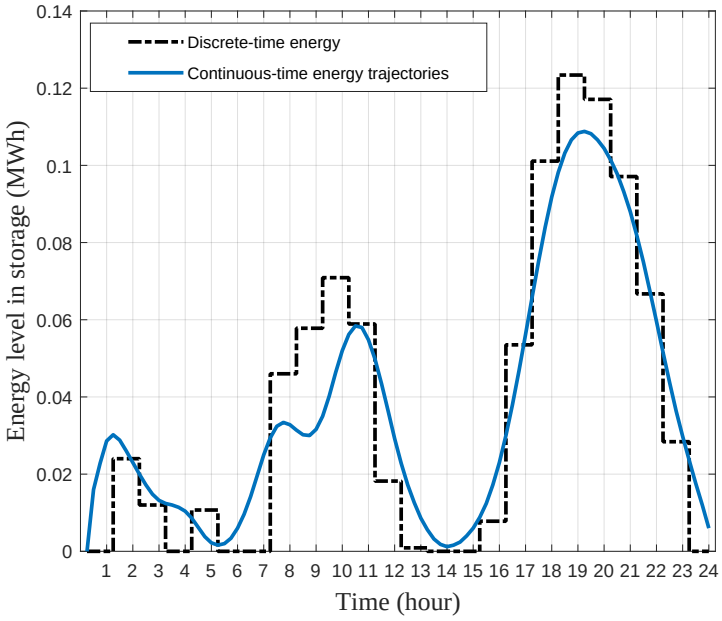

Figure 9: Energy level in energy storage

reserve market of the discrete-time model. In contrast, the day-ahead operation of the continuous-time model is smooth which leads to smoother operation in the real-time reserve market that is illustrated in Fig. 10. Due to the smooth operation schedule of day-ahead continuous-time model, the lower jumps in the reserve gate of continuous-time modeling reduces the ramping events and lower required flexibility in reserve market. Besides, regarding Fig. 10, it can be concluded that the classic discrete-time model's piece-wise constant load profile in day-ahead excludes a large portion of net-load for reserve operation, which requires more flexibility during the reserve market.

6.1.4. IGDT-based risk assessment

The IGDT method is used as a classical approach to determine the impact of robustness and opportunistic uncertainties. The uncertainty of wind energy is the most important uncertainty in this paper. The results of the applied IGDT method on both discrete-time and continuous-time models are represented in

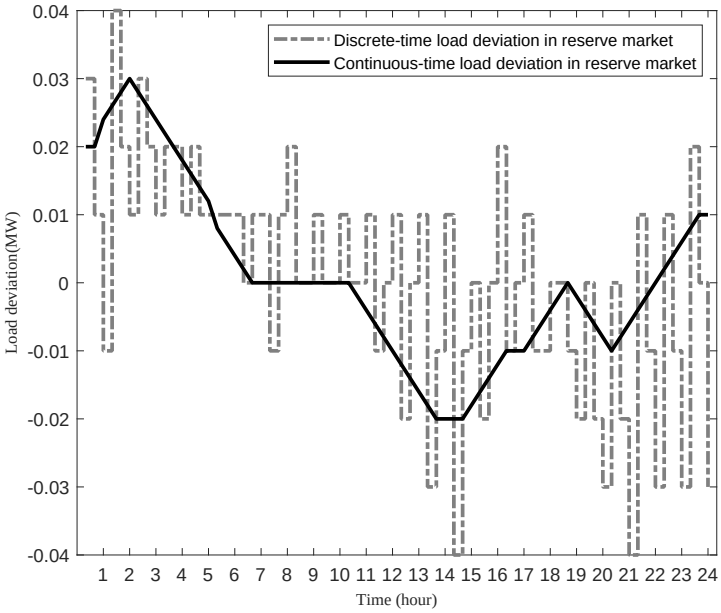

Figure 10: Load deviation in real-time reserve market

Table 2. According to Table II, it can be shown that for a \$10 increment of the cost compared to base costs \$993 and \$984, the maximum amount of *RO* is 0.39 and 1.58 for discrete-time and continuous-time models and that indicates the more robustness of continuous-time model against the uncertainty of wind energy. The results of the \$50 and \$100 cost increment confirm the robustness feature of the continuous-time model in the comparison of the discrete-time model. The results of the opportunity problem on the IGDT technique represent the more opportunistic nature of the continuous-time model compared to the discrete-time procedure. For example, for \$50 cost reduction, the discrete-time model needs to minimum 293% increment in the wind power. In contrast, the continuous-time model can reduce the cost with a minimum 21% wind power increment. From the obtained results if IGDT technique some points can be concluded for effective impacts of continuous-time modeling on uncertainty modeling of proposed test system. First, the flexible operation of using in EDHS can help in flexible performance of variables under the uncertain parameters of

Table 2: The results of applied IGDT technique

Robustness	Discrete-time	RO	0.39	1.02	1.02
		cost	1003	1124.83	1103
	Continuous-time	RO	1.58	1.95	1.95
		cost	994	935.95	1094
Opportunistic	Discrete-time	OP	0.45	2.93	5.49
		cost	983	884.83	883
	Continuous-time	OP	0.10	0.21	1.51
		cost	974	815.95	874

the optimization problem. Second, the chosen time intervals with the continuity conditions help the system in having the higher variables and opportunity to have flexible performance under the uncertain operation modeled by IGDT.

6.2. Model validation

In order to validate the proposed system, the system performance under other load data is investigated. The new continuous and discrete-time load profiles used in validation are represented in Fig. 11. From the system components, the operation of energy storage devices and heat pumps are chosen to be investigated. The continuous-time and discrete-time operation of energy storage device is represented in Fig. 12. According to this figure, both the continuous-time and discrete-time operation are equivalent that means the correct operating of the model. From Fig. 12 it can be shown that the storage device has a huge jumps under the new load profiles represented in Fig. 11. Besides, the operation of heat pump under the new load profile is represented in Fig. 13. Fewer operation of heat pumps under the discrete-time model of new load profiles is illustrated in Fig. 13. The reason for this fewer operating power of heat pump could be related to difference in operating power of energy storage in both continuous-time and discrete-time new load profiles.

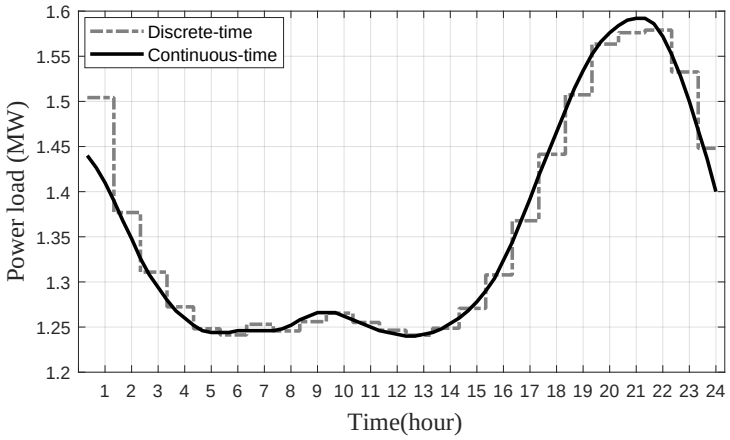

Figure 11: New continuous and discrete-time load profile

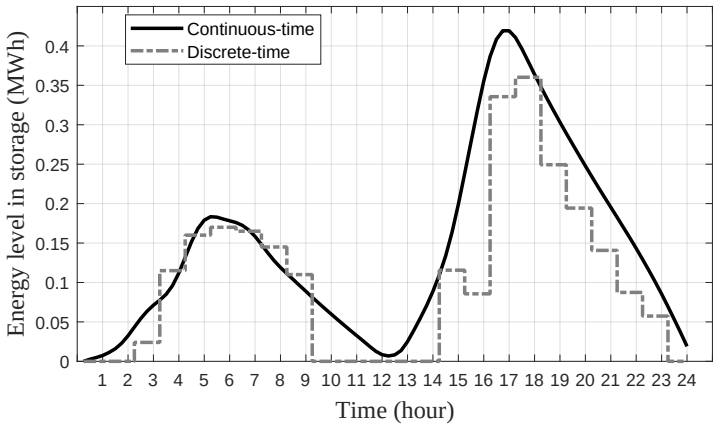

Figure 12: Operation of energy storage under new load profile

7. Conclusion

Linking electricity and district heating networks with energy storage devices provides essential flexibility services, including regulatory reserve, in power system operation, which might enhance the reliability and cost-effectiveness of systems with a high penetration of renewable energy resources. Using an appropriate optimization approach could model and measure the flexibility resulting from the integrated system in the presence of different electricity markets. In

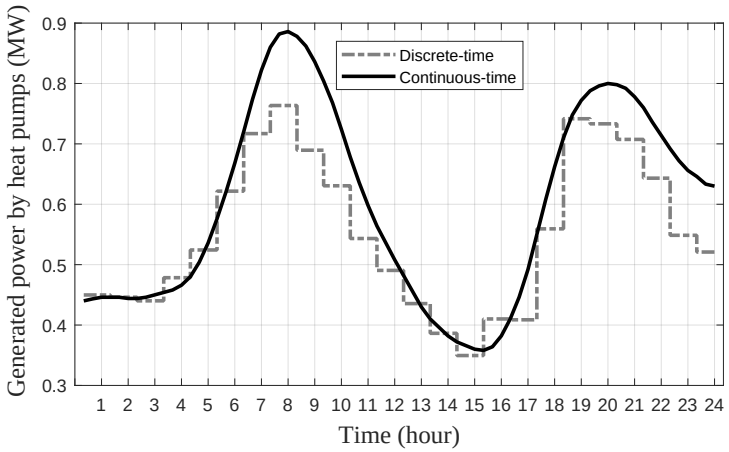

Figure 13: Operation of heat pump under new load profile

this paper, continuous-time optimization is proposed to model the EDHS. The results indicated that the system cost in the discrete-time and continuous-time models are $993 and $984, respectively, which show a cost reduction of 0.91% in the use of continuous-time modeling strategy. According to the obtained, another advantage of the proposed continuous-time modeling is that it reduces the ramping events of EDHS in the regulation reserve stage. Besides, in the IGDT technique, using the opportunity and robustness functions can be appropriate to investigate the effects of uncertainty. The results of IGDT represent that in the continuous-time method, there are more opportunities and fewer losses compared to the discrete-time modeling strategy. Thus, using the proposed continuous-time optimization gives effective management of uncertainties.

References

[1] J. F. Zhang, X. W. Wu, J. G. Qu, D. W. Zhang, and Z. G. Qu. Electrohydrodynamic and heat transfer characteristics of a planar ionic wind generator with flat electrodes. *Applied Thermal Engineering*, 211:118508, jul 2022.

[2] Bert Kruyt, Michael Lehning, and Annelen Kahl. Potential contributions

of wind power to a stable and highly renewable Swiss power supply. *Applied Energy*, 192:1–11, apr 2017.

[3] Shengli Liao, Huan Liu, Benxi Liu, Hongye Zhao, and Mingqing Wang. An information gap decision theory-based decision-making model for complementary operation of hydro-wind-solar system considering wind and solar output uncertainties. *Journal of Cleaner Production*, 348:131382, may 2022.

[4] Yixiao Han, Yanfen Liao, Xiaoqian Ma, Xing Guo, Changxin Li, and Xinyu Liu. Modeling and optimization of a novel Oxy-fuel/Solar/Wind/Battery power generation system. *Applied Thermal Engineering*, 214:118862, sep 2022.

[5] 20% wind energy by 2030. Increasing wind energy's contribution TO U.S. electricity supply, 2013.

[6] Xiang Li, Qi Gao, Yuying Cao, Yanfei Yang, Shiming Liu, Zhong Lin Wang, and Tinghai Cheng. Optimization strategy of wind energy harvesting via triboelectric-electromagnetic flexible cooperation. *Applied Energy*, 307:118311, feb 2022.

[7] Sukanta Roy, Ranjan Das, and Ujjwal K. Saha. Identification of Geographical Locations to Operate Savonius Wind Turbine Rotor for Meeting a Desired Performance. American Society of Mechanical Engineers, dec 2017. ISBN 978-0-7918-5851-6.

[8] Sukanta Roy, Ranjan Das, and Ujjwal K. Saha. An inverse method for optimization of geometric parameters of a Savonius-style wind turbine. *Energy Conversion and Management*, 155:116–127, jan 2018.

[9] Chao Chen, Ziming Yang, and Guoping Hu. Signalling the cost of intermittency: What is the value of curtailed renewable power? *Journal of Cleaner Production*, 302:126998, jun 2021.

[10] Nan Li, Xunwen Zhao, Xunpeng Shi, Zhenwei Pei, Hailin Mu, and Farhad Taghizadeh-Hesary. Integrated energy systems with CCHP and hydrogen

supply: A new outlet for curtailed wind power. *Applied Energy*, 303:117619, dec 2021.

[11] Yichi Zhang, Pär Johansson, and Angela Sasic Kalagasidis. Feasibilities of utilizing thermal inertia of district heating networks to improve system flexibility. *Applied Thermal Engineering*, 213:118813, aug 2022.

[12] Xinyu Chen, Chongqing Kang, Mark O'Malley, Qing Xia, Jianhua Bai, Chun Liu, Rongfu Sun, Weizhou Wang, and Hui Li. Increasing the Flexibility of Combined Heat and Power for Wind Power Integration in China: Modeling and Implications. *IEEE Transactions on Power Systems*, 30(4): 1848–1857, jul 2015.

[13] Yuchun Li, Jinkuan Wang, Yinghua Han, Qiang Zhao, Xiaohan Fang, and Zhiao Cao. Robust and opportunistic scheduling of district integrated natural gas and power system with high wind power penetration considering demand flexibility and compressed air energy storage. *Journal of Cleaner Production*, 256:120456, may 2020.

[14] Haider Niaz, Jay J. Liu, and Fengqi You. Can Texas mitigate wind and solar curtailments by leveraging bitcoin mining? *Journal of Cleaner Production*, 364:132700, sep 2022.

[15] Rufeng Zhang, Tao Jiang, Wenming Li, Guoqing Li, Houhe Chen, and Xue Li. Day-ahead scheduling of integrated electricity and district heating system with an aggregated model of buildings for wind power accommodation. *IET Renewable Power Generation*, 13(6):982–989, apr 2019.

[16] Wandong Zheng, Jay J. Hennessy, and Hailong Li. Reducing renewable power curtailment and CO ₂ emissions in China through district heating storage. *WIREs Energy and Environment*, 9(1), jan 2020.

[17] Chenhui Lin, Wenchuan Wu, Bin Wang, Mohammad Shahidehpour, and Boming Zhang. Joint Commitment of Generation Units and Heat Exchange

Stations for Combined Heat and Power Systems. *IEEE Transactions on Sustainable Energy*, 11(3):1118–1127, jul 2020.

[18] Ruifeng Cao, Yue Lu, Daren Yu, Yufeng Guo, Weiwei Bao, Zhongbin Zhang, and Chuanxin Yang. A novel approach to improving load flexibility of coal-fired power plant by integrating high temperature thermal energy storage through additional thermodynamic cycle. *Applied Thermal Engineering*, 173:115225, jun 2020.

[19] Jon Gustav Kirkerud, Torjus Folsland Bolkesjø, and Erik Trømborg. Power-to-heat as a flexibility measure for integration of renewable energy. *Energy*, 128:776–784, jun 2017.

[20] Wolf-Peter Schill and Alexander Zerrahn. Flexible electricity use for heating in markets with renewable energy. *Applied Energy*, 266:114571, may 2020.

[21] Zhi Zhou and Audun Botterud. Dynamic scheduling of operating reserves in co-optimized electricity markets with wind power. *IEEE Transactions on Power Systems*, 29(1):160–171, jan 2014.

[22] Hessam Golmohamadi, Kim Guldstrand Larsen, Peter Gjøl Jensen, and Imran Riaz Hasrat. Integration of flexibility potentials of district heating systems into electricity markets: A review. *Renewable and Sustainable Energy Reviews*, 159:112200, may 2022.

[23] Yizhou Zhou, Mohammad Shahidehpour, Zhinong Wei, Zhiyi Li, Guoqiang Sun, and Sheng Chen. Distributionally Robust Co-Optimization of Energy and Reserve for Combined Distribution Networks of Power and District Heating. *IEEE Transactions on Power Systems*, 35(3):2388–2398, may 2020.

[24] Jin Tan, Qiuwei Wu, Qinran Hu, Wei Wei, and Feng Liu. Adaptive robust energy and reserve co-optimization of integrated electricity and heating system considering wind uncertainty. *Applied Energy*, 260:114230, 2020.

[25] Jin Tan, Qiuwei Wu, and Menglin Zhang. Strategic investment for district heating systems participating in energy and reserve markets using heat flexibility. *International Journal of Electrical Power and Energy Systems*, 137, 2022.

[26] Zhigang Li, Wenchuan Wu, Jianhui Wang, Boming Zhang, and Taiyi Zheng. Transmission-Constrained Unit Commitment Considering Combined Electricity and District Heating Networks. *IEEE Transactions on Sustainable Energy*, 7(2):480–492, apr 2016.

[27] Huansheng Zhou, Zhigang Li, J. H. Zheng, Q. H. Wu, and Haibo Zhang. Robust Scheduling of Integrated Electricity and Heating System Hedging Heating Network Uncertainties. *IEEE Transactions on Smart Grid*, 11(2): 1543–1555, mar 2020.

[28] Mosayeb Bornapour, Rahmat-Allah Hooshmand, Amin Khodabakhshian, and Moein Parastegari. Optimal coordinated scheduling of combined heat and power fuel cell, wind, and photovoltaic units in micro grids considering uncertainties. *Energy*, 117:176–189, 2016.

[29] Menglin Zhang, Qiuwei Wu, Jinyu Wen, Bo Pan, and Shiqiang Qi. Two-stage stochastic optimal operation of integrated electricity and heat system considering reserve of flexible devices and spatial-temporal correlation of wind power. *Applied Energy*, 275:115357, 2020.

[30] Mikhail Skalyga and Quiwei Wu. Distributionally Robust Co-Optimization of Energy and Reserve Dispatch of Integrated Electricity and Heat System. In *2020 International Conference on Probabilistic Methods Applied to Power Systems, PMAPS 2020 - Proceedings*. Institute of Electrical and Electronics Engineers Inc., aug 2020. ISBN 9781728128221.

[31] Yizhou Zhou, Mohammad Shahidehpour, Zhinong Wei, Zhiyi Li, Guoqiang Sun, and Sheng Chen. Distributionally Robust Unit Commitment in Coordinated Electricity and District Heating Networks. *IEEE Transactions on Power Systems*, 35(3):2155–2166, may 2020.

[32] Hosein Khorsand and Ali Reza Seifi. Probabilistic energy flow for multi-carrier energy systems. *Renewable and Sustainable Energy Reviews*, 94: 989–997, 2018.

[33] Houhe Chen, Ting Zhang, Rufeng Zhang, Tao Jiang, Xue Li, and Guoqing Li. Interval optimal scheduling of integrated electricity and district heating systems considering dynamic characteristics of heating network. *IET Energy Systems Integration*, 2(3):179–186, sep 2020.

[34] Nur Alom, Ranjan Das, and Ujjwal K. Saha. Optimization of Aerodynamic Parameters of an Elliptical-Bladed Savonius Wind Rotor Using Multi-Objective Genetic Algorithms. American Society of Mechanical Engineers, dec 2019. ISBN 978-0-7918-8353-2.

[35] Biplab Kumar Debnath and Ranjan Das. Prediction of performance coefficients of a three-bucket Savonius rotor using artificial neural network. *Journal of Renewable and Sustainable Energy*, 2(4):043107, jul 2010.

[36] Masood Parvania and Anna Scaglione. Unit Commitment with Continuous-Time Generation and Ramping Trajectory Models. *IEEE Transactions on Power Systems*, 31(4):3169–3178, jul 2016.

[37] Masood Parvania and Roohallah Khatami. Continuous-time marginal pricing of electricity. *IEEE Transactions on Power Systems*, 32(3):1960–1969, may 2017.

[38] Roohallah Khatami and Masood Parvania. Continuous-Time Locational Marginal Price of Electricity. *IEEE Access*, 7:129480–129493, 2019.

[39] Avishan Bagherinezhad, Roohallah Khatami, and Masood Parvania. Continuous-time look-ahead flexible ramp scheduling in real-time operation. *International Journal of Electrical Power and Energy Systems*, 119: 105895, jul 2020.

[40] Bosong Li, Avishan Bagherinezhad, Roohallah Khatami, and Masood Parvania. Continuous-Time Look-Ahead Optimization of Energy Storage in

Real-Time Balancing and Regulation Markets. *IEEE Systems Journal*, pages 1–8, jul 2020.

[41] Roohallah Khatami, Masood Parvania, and Akil Narayan. Flexibility Reserve in Power Systems: Definition and Stochastic Multi-Fidelity Optimization. *IEEE Transactions on Smart Grid*, 11(1):644–654, jan 2020.

[42] Ahmad Nikoobakht, Jamshid Aghaei, Miadreza Shafie-Khah, and João P.S. Catalão. Continuous-Time Co-Operation of Integrated Electricity and Natural Gas Systems with Responsive Demands under Wind Power Generation Uncertainty. *IEEE Transactions on Smart Grid*, 11(4):3156–3170, jul 2020.

[43] Helge Averfalk, Paul Ingvarsson, Urban Persson, and Sven Werner. On the use of surplus electricity in district heating systems, 2014.

[44] Satu Paiho and Francesco Reda. Towards next generation district heating in Finland. *Renewable and Sustainable Energy Reviews*, 65:915–924, nov 2016.

[45] Peter Lorenzen and Carlos Alvarez-Bel. Variable cost evaluation of heating plants in district heating systems considering the temperature impact. *Applied Energy*, 305:117909, jan 2022.

[46] Ramin Nourollahi, Pouya Salyani, Kazem Zare, Behnam Mohammadi-Ivatloo, and Zulkurnain Abdul-Malek. Peak-Load Management of Distribution Network Using Conservation Voltage Reduction and Dynamic Thermal Rating. *Sustainability*, 14(18):11569, sep 2022.

[47] Pouya Salyani, Ramin Nourollahi, Kazem Zare, and Reza Razzaghi. A new MILP model of switch placement in distribution networks with consideration of substation overloading during load transfer. *Sustainable Energy, Grids and Networks*, 32:100944, dec 2022.

[48] Ramin Nourollahi, Reza Gholizadeh-Roshanagh, Hamideh Feizi-Aghakandi, Kazem Zare, and Behnam Mohammadi-Ivatloo. Power

Distribution Expansion Planning in the Presence of Wholesale Multimarkets. *IEEE Systems Journal*, pages 1–10, 2022.

[49] Yizhou Zhou, Mohammad Shahidehpour, Zhinong Wei, Zhiyi Li, Guoqiang Sun, and Sheng Chen. Distributionally Robust Unit Commitment in Coordinated Electricity and District Heating Networks. *IEEE Transactions on Power Systems*, 35(3):2155–2166, may 2020.

[50] Kazem Zare, Mohsen Parsa Moghaddam, and Mohammad Kazem Sheikh-El-Eslami. Risk-based electricity procurement for large consumers. *IEEE Transactions on Power Systems*, 26(4):1826–1835, 2011.

[51] L. B. W. and P. M. Prenter. *Splines and Variational Methods.*, volume 56. Courier Corporation, 1991.